Comparison of Baseline Signal Correction Methods for Dynamic Contrast Enhanced MRI

Y. Xue[1], M. A. Rosen[1], and H. Song[1]
[1]Radiology, University of Pennsylvania, Philadelphia, PA, United States

Introduction: Dynamic contrast-enhanced (DCE)-MRI has emerged as a valuable tool for evaluating tumor vascular response and assessment of antiangiogenic and antivascular therapeutics. To measure the perfusion parameters, such as K^{trans}, the observed signal intensity changes need to be converted to gadolinium concentration and subsequently fit to the pharmacokinetic model. This conversion relies on accurate mapping of baseline (pre-contrast) AIF (arterial input function) and tumor signal. As the T_1 of blood (~1200ms) and tissues (~500-1000ms) are much longer than the TRs used in DCE-MRI (<4ms), the SNR of the pre-contrast signal can sometimes be very low particularly at higher spatial resolutions, causing noise to dominate the measured intensity. In this abstract, we compare three different methods of baseline signal correction to determine which method best improves the estimation of K^{trans}.

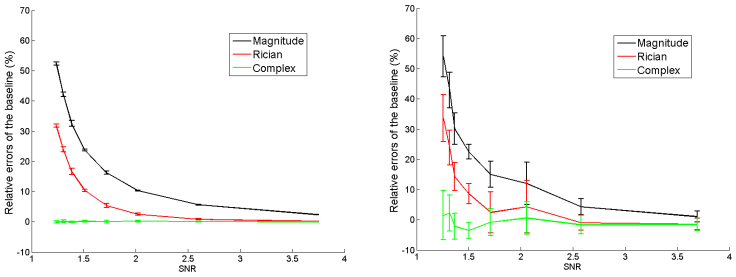

Large ROI Small ROI

Figure 1. The relative errors (mean±SD) of the baseline signals to the true value for the three correction methods: 1. Magnitude averaging (black), 2. Rician correction (red), 3. Complex averaging (green). Different ROI sizes for the AIF (Large ROI: 34-pixel diameter, small ROI: 5-pixel diameter) were used to demonstrate the size effect on the different methods.

Methods: Simulation experiments were performed to evaluate the performance of different baseline correction methods. A modified Shepp-Logan phantom consisting of three circular regions (one tumor and two AIFs of different sizes) was used. AIF signal was simulated using an experimentally-derived model [1]. Tumor signal was subsequently generated using Toft's model with K^{trans} of 0.4 and Ve of 0.2. K-space data were generated analytically for the Golden angle radial acquisition scheme [2]. Normally distributed zero-mean noises with different standard deviations were added to examine the performance at different SNRs. The dynamic data were reconstructed using a K-space-weighted image contrast (KWIC) filter, as is done in current studies to achieve higher effective temporal resolution [3]. The centermost region of the KWIC k-space was filled with 25 views, yielding an effective temporal resolution of 2 sec, assuming a 3D hybrid radial sequence with TR=3.2ms and 26 slices. The low SNR baseline AIF and tumor signals were corrected spatially and temporally using the following three methods. (1) Magnitude averaging. The magnitude signals were averaged spatially (within ROI) and temporally (all baseline time points (2 min pre-contrast was assumed)). The baseline signals were subsequently replaced by the single corrected baseline value. (2) Rician correction [4]. The mean (M) and standard deviation (σ) of magnitude baseline signals within ROI were calculated and the baseline was corrected using the equation:

$$\tilde{A} = \sqrt{|M^2 - \sigma^2|} \qquad (1).$$

Where $\tilde{A}$ is Rician corrected baseline signal. (3) Complex averaging. For this method, complex KWIC images were reconstructed instead of magnitude images. The complex baseline signals were averaged spatially and temporally before converting to magnitude. For the non-baseline time points (during and following contrast injection), the AIF and tumor signals were corrected by using averaged magnitude or complex data within each ROI by the corresponding methods. No temporal averaging was applied. The gadolinium concentration curves were converted from the corrected AIF and tumor curves and K^{trans} was calculated and compared with the true value.

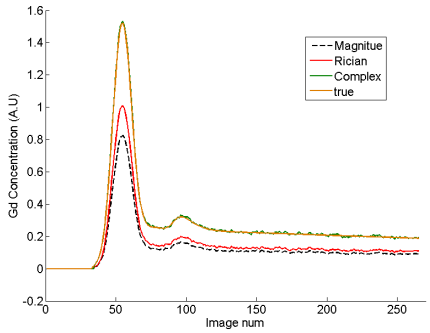

Figure 2. Gad concentration curves converted from the AIF signals (larger ROI) using different correction methods for SNR = 1.7. The true and complex averaging curves overlap.

Results: Figure 1 shows the errors in the baseline signal intensities of the AIF relative to the true value at various SNR levels. The SNR was defined as the mean of the AIF region divided by the mean of the background from baseline KWIC images. As expected, at higher SNRs (above 3 or so) all methods yield values close to the true value. At lower SNRs, significant errors are generated using the conventional magnitude or Rician corrected methods. In contrast, complex averaging provided accurate estimation of the true baseline signal at all SNRs for the larger ROI, although variances were higher at lower SNRs for the smaller ROI. Figure 2 shows the AIF concentration curves converted from the corrected AIF signals. The error in the peak AIF was up to 50% of the true value for the magnitude averaged signal at SNR of 1.7. Figure 3 shows the resulting errors in the computed tumor K^{trans} values. The figure shows that the complex averaging method provided accurate estimation of K^{trans} even at lower SNRs while large errors can result with magnitude averaging and somewhat reduced errors with Rician correction.

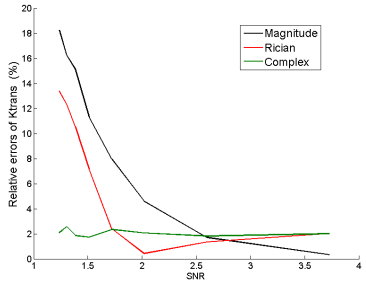

Figure 3. The relative errors of the K^{trans} using the larger AIF for the three correction methods: 1.Magnitude averaging (black), 2. Rician correction (red), 3. Complex averaging (green).

Discussion and Conclusion: Perfusion parameters are particularly sensitive to the accuracy of the baseline signal, as this value is used to normalize the rest of the curve. We have shown that by acquiring sufficient amount of baseline data, much of the noise can be effectively reduced by averaging of the complex data, particularly for larger ROIs. Although we have evaluated radial acquisition methods, same corrections could be applied for standard Cartesian techniques, if raw data is available. In the absence of complex data, Rician correction could be used to improve the accuracy of lesion perfusion measurements.

Acknowledgments: American Cancer Society RSG-08-118-01-CCE; NIH P41-RR02305; NIH R01-CA125226.

References: ***1.*** Parker et al. Magn Reson Med 2006; 56: 993-1000. ***2.*** Winkelmann et al. IEEE Trans Med Imaging. 2007; 26: 68-76. ***3.*** Song et al. Magn Reson Med 2004; 52: 815-824. ***4.*** Gudbjartsson et al. Magn Reson Med 1995; 34: 910-914.